CHALMERS | GÖTEBORG UNIVERSITY

PREPRINT 2008:10

A Posteriori Error Estimates for Continuous/Discontinuous Galerkin Approximations of the Kirchhoff-Love Plate

PETER HANSBO
MATS G. LARSON

Department of Mathematical Sciences
Division of Mathematics
CHALMERS UNIVERSITY OF TECHNOLOGY
UNIVERSITY OF GOTHENBURG
Göteborg Sweden 2008

Preprint 2008:10

A Posteriori Error Estimates for Continuous/Discontinuous Galerkin Approximations of the Kirchhoff-Love Plate

Peter Hansbo and Mats G. Larson

Department of Mathematical Sciences
Division of Mathematics
Chalmers University of Technology and University of Gothenburg
SE-412 96 Göteborg, Sweden
Göteborg, February 2008

Preprint 2008:10
ISSN 1652-9715

Matematiska vetenskaper
Göteborg 2008

A Posteriori Error Estimates for Continuous/Discontinuous Galerkin Approximations of the Kirchhoff-Love Plate

Peter Hansbo and Mats G. Larson

Abstract

We present energy norm a posteriori error estimates for continuous/discontinuous Galerkin (c/dG) approximations of the Kirchhoff-Love plate problem. The method is based on a continuous displacement field inserted into a symmetric discontinuous Galerkin formulation of the fourth order partial differential equation governing the deflection of a thin plate. We also give explicit formulas for the penalty parameter involved in the formulation.

1 Introduction

Thin plates are modeled by fourth order differential equations according to the Kirchhoff-Love theory and thus standard finite element methods require C^1–continuous finite element spaces. Such spaces are difficult to construct on unstructured meshes. Some possibilities are: the C^1 Argyris element which involves polynomials of order five and macro element techniques involving polynomials of order three, see Ciarlet [6]. Another possibility is to consider nonconforming finite element spaces, for instance, the classical Morley plate element [12]. More recently the continuous/discontinuous Galerkin (c/dG) method was proposed by Engel et al. [8]. Here a standard continuous piecewise polynomial space of order greater or equal to two is inserted into a discontinuous Galerkin formulation of the fourth order plate equation. This formulation has the advantage that it uses standard finite element spaces, is easy to implement, and extends naturally to higher order polynomials. A more general formulation allowing fully discontinuous piecewise polynomial approximation was proposed and analyzed in [9]. We also mention the related classical paper by Baker [1] where a discontinuous Galerkin method for higher order partial differential equations was first introduced and the recent work by Wells and Dung [15] where a modified c/dG method plate approximations based on lifting operators is presented.

In this paper we prove an a posteriori error estimate in the energy norm for the c/dG method for the Kirchhoff-Love plate. The proof is based on a Helmholtz decomposition for second order tensor fields presented in a recent paper by Beirão da Veiga et al [3] where an a posteriori error estimate for the Morley element was proved. Furthermore, we employ

some technical tools from Larson and Målqvist [10]. We also mention early works on a posteriori error estimates for discontinuous Galerkin methods [2] and for nonconforming methods [5] and [7].

The discontinuous Galerkin formulation involves a penalty parameter, which must be chosen large enough to guarantee a coercive bilinear form. We give explicit lower bounds on the penalty parameter and study the dependency of the error on the penalty parameter. The accuracy in the c/dG method with quadratic polynomials is also compared with the classical nonconforming Morley element.

The paper is organized as follows: in Section 2 we present the Kirchhoff-Love plate model and the continuous/discontinuous Galerkin method, in Section 3 we derive the a posteriori error estimate, and in Section 4 we present some numerical results.

2 The Plate Model and Finite Element Method

2.1 The Kirchoff-Love Plate Model

The clamped Kirchoff-Love plate model takes the form: given f, find the displacement u such that

$$\text{div } \mathbf{div}\, \boldsymbol{\sigma}(\nabla u) = f \quad \text{in } \Omega \tag{1}$$

$$u = 0 \quad \text{on } \partial\Omega \tag{2}$$

$$n \cdot \nabla u = 0 \quad \text{on } \partial\Omega \tag{3}$$

where

$$\boldsymbol{\sigma}(\boldsymbol{\theta}) = 2\mu\boldsymbol{\varepsilon}(\boldsymbol{\theta}) + \lambda\nabla \cdot \boldsymbol{\theta}\, \boldsymbol{I} \tag{4}$$

with $\mu = E/(24(1+\nu))$, and $\lambda = \nu E/(12(1-\nu^2))$, where the material constants E and ν are the Young's modulus and Poisson's ratio, respectively, $\boldsymbol{\sigma}$ is the moment tensor, and $\boldsymbol{\varepsilon}$ is the curvature tensor with components

$$\varepsilon_{ij}(\boldsymbol{\theta}) = \frac{1}{2}\left(\frac{\partial \theta_i}{\partial x_j} + \frac{\partial \theta_j}{\partial x_i}\right)$$

We also use the notation

$$\text{div } \boldsymbol{\theta} = \frac{\partial \theta_1}{\partial x_1} + \frac{\partial \theta_2}{\partial x_2}, \quad \mathbf{div}\, \boldsymbol{\sigma} = \begin{bmatrix} \dfrac{\partial \sigma_{11}}{\partial x_1} + \dfrac{\partial \sigma_{12}}{\partial x_2} \\ \dfrac{\partial \sigma_{21}}{\partial x_1} + \dfrac{\partial \sigma_{22}}{\partial x_2} \end{bmatrix}$$

The corresponding variational formulation reads: find the displacement $u \in H_0^2(\Omega)$ such that

$$a(\nabla u, \nabla v) = (f, v) \quad \forall v \in H_0^2(\Omega) \tag{5}$$

Here the bilinear form $a(\cdot,\cdot)$ is defined by

$$a(\boldsymbol{\theta},\boldsymbol{\vartheta}) = (\boldsymbol{\sigma}(\boldsymbol{\theta}),\boldsymbol{\varepsilon}(\boldsymbol{\vartheta}))$$

where $(\cdot,\cdot)$ is the $L^2(\Omega)$ inner product.

Finally, we remark that since our discrete method employs subspaces of $H_0^1(\Omega)$ rather than of $H_0^2(\Omega)$, we will in the following assume that $f \in H^{-1}(\Omega)$. Note however, that this is a technical assumption; since our discrete method is $C^0(\Omega)$–continuous, point loads are not excluded (though they are indeed not in $H^{-1}(\Omega)$) and are used in the numerical examples.

2.2 The Continuous/Discontinuous Galerkin Method

We consider a subdivision $\mathcal{T} = \{T\}$ of Ω into a geometrically conforming finite element mesh. We assume that the elements are shape regular, i.e., the quotient of the diameter of the smallest circumscribed sphere and the largest inscribed sphere is uniformly bounded. We denote by h_T the diameter of element T and by $h = \max_{T\in\mathcal{T}} h_T$ the global mesh size parameter. We shall use continuous, piecewise polynomial, approximations of the transverse displacement:

$$\mathcal{CP}_k = \{v \in C^0(\Omega) : \ v|_T \in \mathcal{P}_k(T)\ \forall T \in \mathcal{T}\}$$

where $\mathcal{P}_k(T)$ is the space of polynomials of order $k \geq 2$ defined on T. Furthermore, we let $\mathcal{CP}_{k,0} = \mathcal{CP}_k \cap H_0^1$.

We introduce the Scott-Zhang interpolation operator $\pi : H_0^1(\Omega) \to \mathcal{CP}_{k,0}$ and recall the following elementwise interpolation error estimate

$$|u - \pi u|_{T,m} \leq C h_T^{s-m} |u|_{\mathcal{N}(T),s} \tag{6}$$

where $0 \leq m \leq s \leq k+1$ and $\mathcal{N}(T)$ is the union of all elements which are neighbors to T, cf. [4].

To define our method we introduce the set of edges in the mesh, $\mathcal{E} = \{E\}$, and we split $\mathcal{E}$ into two disjoint subsets

$$\mathcal{E} = \mathcal{E}_I \cup \mathcal{E}_B$$

where $\mathcal{E}_I$ is the set of edges in the interior of Ω and $\mathcal{E}_B$ is the set of edges on the boundary. Further, with each edge we associate a fixed unit normal $\boldsymbol{n}$ such that for edges on the boundary $\boldsymbol{n}$ is the exterior unit normal. We denote the jump of a function $\boldsymbol{v} \in \boldsymbol{\Gamma}_h$ at an edge E by $[\boldsymbol{v}] = \boldsymbol{v}^+ - \boldsymbol{v}^-$ for $E \in \mathcal{E}_I$ and $[\boldsymbol{v}] = \boldsymbol{v}^+$ for $E \in \mathcal{E}_B$, and the average $\langle \boldsymbol{v} \rangle = (\boldsymbol{v}^+ + \boldsymbol{v}^-)/2$ for $E \in \mathcal{E}_I$ and $\langle \boldsymbol{v} \rangle = \boldsymbol{v}^+$ for $E \in \mathcal{E}_B$, where $\boldsymbol{v}^\pm = \lim_{\epsilon \downarrow 0} \boldsymbol{v}(\boldsymbol{x} \mp \epsilon\, \boldsymbol{n})$ with $\boldsymbol{x} \in E$.

Our method can now be formulated as follows: find $U \in \mathcal{CP}_{k,0}$ such that

$$a_h(\nabla U, \nabla v) = (f, v) \quad \forall v \in \mathcal{CP}_{k,0} \tag{7}$$

The bilinear form $a_h(\cdot,\cdot)$ is defined by

$$\begin{aligned} a_h(\boldsymbol{\theta},\boldsymbol{\vartheta}) &= \sum_{T\in\mathcal{T}}(\boldsymbol{\sigma}(\boldsymbol{\theta}),\boldsymbol{\varepsilon}(\boldsymbol{\vartheta}))_T \\ &\quad - \sum_{E\in\mathcal{E}_I\cup\mathcal{E}_B}\Big((\langle \boldsymbol{n}\cdot\boldsymbol{\sigma}(\boldsymbol{\theta})\rangle,[\boldsymbol{\vartheta}])_E + ([\boldsymbol{\theta}],\langle \boldsymbol{n}\cdot\boldsymbol{\sigma}(\boldsymbol{\vartheta})\rangle)_E\Big) \\ &\quad +\gamma\sum_{E\in\mathcal{E}_I\cup\mathcal{E}_B} h_E^{-1}([\boldsymbol{\theta}],[\boldsymbol{\vartheta}])_E \end{aligned} \tag{8}$$

for all $\boldsymbol{\theta},\boldsymbol{\vartheta}\in\bigoplus_{T\in\mathcal{T}}[H^1(T)]^2$. Here

$$\gamma = k^2\left(2\mu+2\lambda\right)\gamma_0 \tag{9}$$

where γ_0 is a positive dimensionless parameter, and h_E is defined by

$$h_E = \left(|T^+|+|T^-|\right)/|E| \quad \text{for } E=\partial T^+\cap\partial T^- \tag{10}$$

with $|T|$ the area of T, on each edge E.

Remark 2.1 *The form* (8) *is the one used in the analysis below. However, since the tangential derivative along an edge between two elements is continuous, we may alternatively use the form*

$$\begin{aligned} a_h^*(\boldsymbol{\theta},\boldsymbol{\vartheta}) &= \sum_{T\in\mathcal{T}}(\boldsymbol{\sigma}(\boldsymbol{\theta}),\boldsymbol{\varepsilon}(\boldsymbol{\vartheta}))_T \\ &\quad - \sum_{E\in\mathcal{E}_I\cup\mathcal{E}_B}\Big((\langle \boldsymbol{n}\cdot\boldsymbol{\sigma}(\boldsymbol{\theta})\cdot\boldsymbol{n}\rangle,[\boldsymbol{n}\cdot\boldsymbol{\vartheta}])_E + ([\boldsymbol{n}\cdot\boldsymbol{\theta}],\langle \boldsymbol{n}\cdot\boldsymbol{\sigma}(\boldsymbol{\vartheta})\cdot\boldsymbol{n}\rangle)_E\Big) \\ &\quad +\gamma\sum_{E\in\mathcal{E}_I\cup\mathcal{E}_B} h_E^{-1}([\boldsymbol{n}\cdot\boldsymbol{\theta}],[\boldsymbol{n}\cdot\boldsymbol{\vartheta}])_E \end{aligned} \tag{11}$$

This form was used in all numerical examples.

The coercivity of the discrete operator and convergence of the method follows from the general analysis given in [9]. We shall here restrict ourselves to a more detailed discussion on the size of the parameter γ_0 required to ensure coercivity.

2.3 Lower Bound on the Penalty Parameter

In order to show that the method (7) is stable, one must show that $a_h(\cdot,\cdot)$ is coercive with respect to the norm $|||\cdot|||$ defined in (15), which requires that γ_0 is chosen large enough. We shall here instead use of the alternative form $a_h^*(\cdot,\cdot)$, however, since this leads to a sharper estimate for γ_0. Coercivity then hinges on the following inverse inequality (see [9] for details).

Lemma 2.2 *For $v \in P_k(T)$ there is a constant C_{I}, independent of the diameter h, λ, μ, and k, such that*

$$\frac{h_E}{k^2\,(2\mu+2\lambda)}\|\boldsymbol{n}\cdot\boldsymbol{\sigma}(\nabla v)\cdot\boldsymbol{n}\|^2_{L^2(E)} \le C_{\mathrm{I}}\,(\boldsymbol{\sigma}(\nabla v),\boldsymbol{\varepsilon}(\nabla v))_T \tag{12}$$

for E a side of T. If, in addition, T is a affine triangle, C_{I} is also independent of the minimal angle of the triangle T.

We note that this Lemma is a variant of standard inverse inequalities, cf. Ciarlet [6] or Warburton and Hesthaven [14] (where the exact value for a constant like C_{I} is computed in a simple case). Here, however, we also need to take into account the material data. To this end, we invert the stress-strain relation to yield

$$\boldsymbol{\varepsilon} = \frac{1}{2\mu}\left(\boldsymbol{\sigma} - \frac{\lambda}{2\lambda+2\mu}\mathrm{tr}\,\boldsymbol{\sigma}\,\boldsymbol{I}\right) = \frac{1}{2\mu}\boldsymbol{\sigma}^D + \frac{1}{4\lambda+4\mu}\mathrm{tr}\,\boldsymbol{\sigma}\,\boldsymbol{I}$$

where $\boldsymbol{\sigma}^D := \boldsymbol{\sigma} - \mathrm{tr}\,\boldsymbol{\sigma}\,\boldsymbol{I}/2$ and $\mathrm{tr}\,\boldsymbol{\sigma} := \sigma_{11}+\sigma_{22}$, and thus we have that

$$\boldsymbol{\sigma}:\boldsymbol{\varepsilon} = \frac{1}{2\mu}\boldsymbol{\sigma}^D:\boldsymbol{\sigma}^D + \frac{1}{4\lambda+4\mu}(\mathrm{tr}\,\boldsymbol{\sigma})^2$$

and

$$\boldsymbol{\sigma}:\boldsymbol{\sigma} = \boldsymbol{\sigma}^D:\boldsymbol{\sigma}^D + \frac{1}{2}(\mathrm{tr}\,\boldsymbol{\sigma})^2$$

so that

$$\boldsymbol{\sigma}:\boldsymbol{\sigma} \le (2\mu+2\lambda)\,\boldsymbol{\sigma}:\boldsymbol{\varepsilon} \tag{13}$$

which explains the scaling in terms of material data between the left and right hand sides of (12).

We shall now calculate upper bounds of the constant C_{I}. Notice that C_{I} is the maximum eigenvalue of the problem

$$A\hat{\boldsymbol{v}} = \omega B\hat{\boldsymbol{v}}, \tag{14}$$

where $\hat{\boldsymbol{v}}$ denotes the coordinates of v in a basis $\{\varphi_j\}$ for $P^k(T)$,

$$A_{ij} = \frac{h_E}{k^2\,(2\mu+2\lambda)}(\boldsymbol{n}\cdot\boldsymbol{\sigma}(\nabla\varphi_i)\cdot\boldsymbol{n}, \boldsymbol{n}\cdot\boldsymbol{\sigma}(\nabla\varphi_j)\cdot\boldsymbol{n})_E$$

and

$$B_{ij} = (\boldsymbol{\sigma}(\nabla\varphi_i),\boldsymbol{\varepsilon}(\nabla\varphi_j))_T$$

Solving this eigenvalue problem numerically gives the values for C_{I} shown in Table 1, using $h_E = 2|T|/|E|$ (the shortest distance from the line defined by the edge to the node not on the edge).

Finally, in order to have coercivity, we need to set $\gamma_0 > 3C_{\mathrm{I}}$, cf. [9].

Remark 2.3 *Table 1 suggests the relation*

$$C_{\mathrm{I},k+1} = \frac{k^2}{k^2-1}C_{\mathrm{I},k}$$

which asymptotically gives $C_{\mathrm{I}} = 1/2$.

k	2	3	4	5	6
C_{I}	1/4	1/3	3/8	2/5	5/12

Table 1: Inverse inequality constant for increasing polynomial degree.

3 An Energy Norm A Posteriori Error Estimate

We introduce the following norm

$$|||v|||^2 = \sum_{T\in\mathcal{T}} (\boldsymbol{\sigma}(\nabla v), \boldsymbol{\varepsilon}(\nabla v))_T \tag{15}$$

on $H_0^2 \cup \mathcal{CP}_{k,0}$. We shall use the following Helmholtz decomposition of 2×2 tensor fields, introduced in [3].

Lemma 3.1 *Let $\boldsymbol{\chi} \in L^2(\Omega, \mathbf{R}^{2\times 2})$ be a second order tensor field. Then there exist $\psi \in H_0^2(\Omega)$, $\rho \in L^2(\Omega)$, and $\boldsymbol{\phi} \in [H^1(\Omega)]^2$ such that*

$$\boldsymbol{\chi} = \boldsymbol{\sigma}(\nabla\psi) + \boldsymbol{\rho} + \mathbf{Curl}\ \boldsymbol{\phi} \tag{16}$$

where

$$\boldsymbol{\rho} = \begin{bmatrix} 0 & -\rho \\ \rho & 0 \end{bmatrix}, \quad \mathbf{Curl}\ \boldsymbol{\phi} = \begin{bmatrix} -\dfrac{\partial\phi_1}{\partial x_2} & \dfrac{\partial\phi_1}{\partial x_1} \\ -\dfrac{\partial\phi_2}{\partial x_2} & \dfrac{\partial\phi_2}{\partial x_1} \end{bmatrix}, \tag{17}$$

and the following stability estimate holds

$$\|\psi\|_2 + \|\rho\| + \|\boldsymbol{\phi}\|_1 \le C\|\boldsymbol{\chi}\|. \tag{18}$$

For a proof, see [3].

We are now ready to formulate our main result. In the following, C denotes a generic constant independent of the meshsize, not necessarily the same at different instances.

Theorem 3.2 *The following a posteriori error estimate holds*

$$|||u - U|||^2 \le C \sum_{T\in\mathcal{T}} \eta_T^2 \tag{19}$$

where the element indicator η_T is defined by

$$\begin{aligned} \eta_T^2 = {} & h_T^4 \|f - \operatorname{div}\ \mathbf{div}\ \boldsymbol{\sigma}(\nabla U)\|_T^2 + h_T^3 \|[\boldsymbol{n}\cdot\mathbf{div}\ \boldsymbol{\sigma}(\nabla U)]\|_{\partial T}^2 \\ & + h_T \|[\boldsymbol{n}\cdot\boldsymbol{\sigma}(\nabla U)]\|_{\partial T}^2 + \gamma^2 h_E^{-1} \|[\nabla U]\|_{\partial T}^2 \end{aligned} \tag{20}$$

Proof. Letting $e = u - U$ be the error and using the Helmholtz decomposition with $\boldsymbol{\chi} = \boldsymbol{\sigma}(\nabla e)$ and elementwise applied derivatives we obtain

$$
\begin{aligned}
|||e|||^2 &= \sum_{T\in\mathcal{T}} (\boldsymbol{\sigma}(\nabla e), \boldsymbol{\varepsilon}(\nabla e))_T && (21)\\
&= \sum_{T\in\mathcal{T}} (\boldsymbol{\varepsilon}(\nabla e), \boldsymbol{\sigma}(\nabla \psi))_T + \sum_{T\in\mathcal{T}} (\boldsymbol{\varepsilon}(\nabla e), \boldsymbol{\rho})_T + \sum_{T\in\mathcal{T}} (\boldsymbol{\varepsilon}(\nabla e), \mathbf{Curl}\ \boldsymbol{\phi})_T && (22)\\
&= I + II + III && (23)
\end{aligned}
$$

We proceed with estimates of the three terms.

Term I. For the first term I we first eliminate the exact solution u using equation (5) and the fact that $\psi \in H_0^2(\Omega)$. Then we use the definition of the finite element method (7) to subtract the Scott-Zhang interpolant $\pi\psi \in \mathcal{CP}_{k,0}$ as follows

$$
\begin{aligned}
I &= \sum_{T\in\mathcal{T}} (\boldsymbol{\sigma}(\nabla e), \boldsymbol{\varepsilon}(\nabla \psi))_T && (24)\\
&= (f, \psi) - \sum_{T\in\mathcal{T}} (\boldsymbol{\sigma}(\nabla U), \boldsymbol{\varepsilon}(\nabla \psi))_T && (25)\\
&= (f, \psi - \pi\psi) - \sum_{T\in\mathcal{T}} (\boldsymbol{\sigma}(\nabla U), \boldsymbol{\varepsilon}(\nabla(\psi - \pi\psi)))_T && (26)\\
&\quad - \sum_{E\in\mathcal{E}_I\cup\mathcal{E}_B} (\langle \boldsymbol{n}\cdot\boldsymbol{\sigma}(\nabla U)\rangle, [\nabla\pi\psi])_E + ([\nabla U], \langle \boldsymbol{n}\cdot\boldsymbol{\sigma}(\nabla\pi\psi)\rangle)_E\\
&\quad + \sum_{E\in\mathcal{E}_I\cup\mathcal{E}_B} \gamma h_E^{-1} ([\nabla U], [\nabla\pi\psi])_E
\end{aligned}
$$

Next, repeated use of Green's formula and observing that

$$
\begin{aligned}
&[\boldsymbol{n}\cdot\boldsymbol{\sigma}(\nabla U)\cdot\nabla(\psi - \pi\psi)] + \langle \boldsymbol{n}\cdot\boldsymbol{\sigma}(\nabla U)\rangle \cdot [\nabla(\pi\psi)]\\
&\qquad = [\boldsymbol{n}\cdot\boldsymbol{\sigma}(\nabla U)\cdot\nabla(\psi - \pi\psi)] - \langle \boldsymbol{n}\cdot\boldsymbol{\sigma}(\nabla U)\rangle \cdot [\nabla(\psi - \pi\psi)]\\
&\qquad = [\boldsymbol{n}\cdot\boldsymbol{\sigma}(\nabla U)] \cdot \langle\nabla(\psi - \pi\psi)\rangle
\end{aligned}
$$

where we used that $[\nabla\pi\psi] = -[\nabla(\psi - \pi\psi)]$, we arrive at

$$
\begin{aligned}
I = &\sum_{T\in\mathcal{T}} (f - \operatorname{div}\,\mathbf{div}\,\boldsymbol{\sigma}(\nabla U), \psi - \pi\psi)_T \\
&+ \sum_{E\in\mathcal{E}_I} ([\boldsymbol{n}\cdot\mathbf{div}\,\boldsymbol{\sigma}(\nabla U)], \psi - \pi\psi)_E \\
&- \sum_{E\in\mathcal{E}_I\cup\mathcal{E}_B} ([\boldsymbol{n}\cdot\boldsymbol{\sigma}(\nabla U)], \langle\nabla(\psi - \pi\psi)\rangle)_E \\
&- \sum_{E\in\mathcal{E}_I\cup\mathcal{E}_B} ([\nabla U], \langle\boldsymbol{n}\cdot\boldsymbol{\sigma}(\nabla\pi\psi)\rangle)_E \\
&+ \sum_{E\in\mathcal{E}_I\cup\mathcal{E}_B} \gamma h_E^{-1}([\nabla U], [\nabla\pi\psi])_E \\
= &\, I_1 + I_2 + I_3 + I_4 + I_5
\end{aligned} \tag{27}
$$

(28)

These five terms may now be directly estimated in a straightforward manner using the Cauchy-Schwartz inequality, the trace inequality

$$\|v\|_{\partial T}^2 \leq C\left(h_T^{-1}\|v\|_T^2 + h_T\|\nabla v\|_T^2\right),$$

cf. Thomée [13], the inverse inequality (12), the interpolation error estimates (6), and finally the stability estimate (18). For convenience we include the estimates.

Term I_1. Using the Cauchy-Schwartz inequality on the sum and scaling with suitable powers of h_T we obtain

$$I_1 = \sum_{T\in\mathcal{T}} (f - \operatorname{div}\,\mathbf{div}\,\boldsymbol{\sigma}(\nabla U), \psi - \pi\psi)_T \tag{29}$$

$$\leq \left(\sum_{T\in\mathcal{T}} h_T^4\|f - \operatorname{div}\,\mathbf{div}\,\boldsymbol{\sigma}(\nabla U)\|_T^2\right)^{1/2} \left(\sum_{T\in\mathcal{T}} h_T^{-4}\|\psi - \pi\psi\|_T^2\right)^{1/2} \tag{30}$$

Next using the interpolation error estimate (6) we have

$$\sum_{T\in\mathcal{T}} h_T^{-4}\|\psi - \pi\psi\|_T^2 \leq C\|\psi\|_2^2 \tag{31}$$

Term I_2. Using the Cauchy-Schwartz inequality on the sum with suitable scaling we get

$$I_2 = \sum_{E\in\mathcal{E}_I} ([\boldsymbol{n}\cdot\mathbf{div}\,\boldsymbol{\sigma}(\nabla U)], \psi - \pi\psi)_E \tag{32}$$

$$\leq \left(\sum_{E\in\mathcal{E}_I} h^3\|[\boldsymbol{n}\cdot\mathbf{div}\,\boldsymbol{\sigma}(\nabla U)]\|_E^2\right)^{1/2} \left(\sum_{E\in\mathcal{E}_I} h^{-3}\|\psi - \pi\psi\|_E^2\right)^{1/2} \tag{33}$$

Using the trace inequality followed by the interpolation error estimate (6) we have

$$\begin{aligned}\sum_{E\in\mathcal{E}_I} h^{-3}\|\psi-\pi\psi\|_E^2 &\leq C\sum_{T\in\mathcal{T}}\left(h^{-4}\|\psi-\pi\psi\|_T^2+h^{-2}\|\nabla(\psi-\pi\psi)\|_T^2\right)\\ &\leq C\|\psi\|_2^2\end{aligned} \tag{34}$$

Term I_3. Using the Cauchy-Schwartz inequality on the sum with suitable scaling we get

$$I_3 = -\sum_{E\in\mathcal{E}_I\cup\mathcal{E}_B}([\boldsymbol{n}\cdot\boldsymbol{\sigma}(\nabla U)],\langle\nabla\psi-\pi\psi\rangle)_E \tag{35}$$

$$\leq\left(\sum_{E\in\mathcal{E}_I\cup\mathcal{E}_B} h\|[\boldsymbol{n}\cdot\boldsymbol{\sigma}(\nabla U)]\|_E^2\right)^{1/2}\left(\sum_{E\in\mathcal{E}_I\cup\mathcal{E}_B} h^{-1}\|\langle\nabla(\psi-\pi\psi)\rangle\|_E^2\right)^{1/2} \tag{36}$$

Using the trace inequality followed by the interpolation error estimate (6) we have

$$\begin{aligned}\sum_{E\in\mathcal{E}_I\cup\mathcal{E}_B} h^{-1}\|\langle\nabla(\psi-\pi\psi)\rangle\|_E^2 &\leq C\sum_{E\in\mathcal{E}_I\cup\mathcal{E}_B}\left(h^{-2}\|\nabla(\psi-\pi\psi)\|_T^2+|\psi-\pi\psi|_{T,2}^2\right)\\ &\leq C\|\psi\|_2^2\end{aligned} \tag{37}$$

Term I_4. Using the Cauchy-Schwartz inequality on the sum with suitable scaling we get

$$I_4 = -\sum_{E\in\mathcal{E}_I\cup\mathcal{E}_B}([\nabla U],\langle\boldsymbol{n}\cdot\boldsymbol{\sigma}(\nabla\pi\psi)\rangle)_E \tag{38}$$

$$\leq\left(\sum_{E\in\mathcal{E}_I\cup\mathcal{E}_B} h_E^{-1}\|[\nabla U]\|_E^2\right)^{1/2}\left(\sum_{E\in\mathcal{E}_I\cup\mathcal{E}_B} h_E\|\langle\boldsymbol{n}\cdot\boldsymbol{\sigma}(\nabla\pi\psi)\rangle\|_E^2\right)^{1/2} \tag{39}$$

Using the inverse inequality and the stability of the interpolation operator π we have

$$\sum_{E\in\mathcal{E}_I\cup\mathcal{E}_B} h_E\|\langle\boldsymbol{n}\cdot\boldsymbol{\sigma}(\nabla\pi\psi)\rangle\|_E^2\leq C\sum_{T\in\mathcal{T}}\|\boldsymbol{\sigma}(\nabla\pi\psi)\|_T^2\leq C\|\psi\|^2 \tag{40}$$

Term I_5. Using the Cauchy-Schwartz inequality on the sum with suitable scaling we get

$$I_5 = \sum_{E\in\mathcal{E}_I\cup\mathcal{E}_B}\gamma h_E^{-1}([\nabla U],[\nabla\pi\psi])_E \tag{41}$$

$$\leq\left(\sum_{E\in\mathcal{E}_I\cup\mathcal{E}_B}\gamma^2 h_E^{-1}\|[\nabla U]\|_E^2\right)^{1/2}\left(\sum_{E\in\mathcal{E}_I\cup\mathcal{E}_B} h_E^{-1}\|[\nabla\pi\psi]\|_E^2\right)^{1/2} \tag{42}$$

Using that $[\nabla\pi\psi]=[\nabla(\pi\psi-\psi)]$ since $\psi\in H_0^2$, the trace inequality, and the interpolation estimate we obtain

$$\sum_{E\in\mathcal{E}_I\cup\mathcal{E}_B} h_E^{-1}\|[\nabla\pi\psi]\|_E^2\leq C\sum_{T\in\mathcal{T}}\left(h_T^{-2}\|\nabla(\psi-\pi\psi)\|_T^2+|\psi-\pi\psi|_{T,2}^2\right)\leq C\|\psi\|_2 \tag{43}$$

Collecting the estimates of I_1–I_5 and using the stability estimate (18) we finally get

$$I\leq C\left(\sum_{T\in\mathcal{T}}\eta_T^2\right)^{1/2}\|\psi\|_2\leq C\left(\sum_{T\in\mathcal{T}}\eta_T^2\right)^{1/2}|||e||| \tag{44}$$

Term *II*. The second term II is zero since $\boldsymbol{\varepsilon}(\nabla e)$ is a symmetric matrix and $\boldsymbol{\rho}$ is anti-symmetric.

Term *III*. To estimate the third term III we first use Green's formula to conclude that

$$III = \sum_{T\in\mathcal{T}} (\boldsymbol{\varepsilon}(\nabla e), \mathbf{Curl}\ \boldsymbol{\phi})_T \tag{45}$$

$$= \sum_{E\in\mathcal{E}} ([\nabla U], \boldsymbol{n}\cdot\mathbf{Curl}\ \boldsymbol{\phi})_E \tag{46}$$

since $\mathbf{div}\ \mathbf{Curl}\ \boldsymbol{\phi} = \mathbf{0}$. Next we note that we can write the right side in the following form

$$III = \sum_{E\in\mathcal{E}} ([\nabla U], \boldsymbol{n}\cdot\mathbf{Curl}\ \boldsymbol{\phi})_E \tag{47}$$

$$= \sum_{T\in\mathcal{T}} (\nabla U - \boldsymbol{w}, \boldsymbol{n}\cdot\mathbf{Curl}\ \boldsymbol{\phi})_{\partial T} \tag{48}$$

for any continuous function $\boldsymbol{w}$ which is zero on the boundary $\partial\Omega$. We can now estimate the contributions from each triangle as follows

$$(\nabla U - \boldsymbol{w}, \boldsymbol{n}\cdot\mathbf{Curl}\ \boldsymbol{\phi})_{\partial T} \leq \|\nabla U - \boldsymbol{w}\|_{\partial T,1/2} \|\boldsymbol{n}\cdot\mathbf{Curl}\ \boldsymbol{\phi}\|_{\partial T,-1/2} \tag{49}$$

Next using the normal trace inequality

$$\|\boldsymbol{n}\cdot\boldsymbol{v}\|_{\partial T,-1/2} \leq C(\|\boldsymbol{v}\|_T + h_T\|\mathrm{div}\ \boldsymbol{v}\|_T) \tag{50}$$

see Larson and Målqvist [10], with $\boldsymbol{v} = \mathbf{curl}\ \phi_i$ for $i = 1, 2$, and the fact that div $\mathbf{curl}\ \phi_i = 0$, we obtain the following inequality

$$\|\boldsymbol{n}\cdot\mathbf{Curl}\ \boldsymbol{\phi}\|_{\partial T,-1/2} \leq C\|\mathbf{Curl}\ \boldsymbol{\phi}\|_T \tag{51}$$

which together with (48) and (49) give

$$III \leq C\left(\sum_{T\in\mathcal{T}} \|\nabla U - \boldsymbol{w}\|^2_{\partial T,1/2}\right)^{1/2} \left(\sum_{T\in\mathcal{T}} \|\mathbf{Curl}\ \boldsymbol{\phi}\|^2_T\right)^{1/2} \tag{52}$$

$$\leq C\left(\sum_{T\in\mathcal{T}} \|\nabla U - \boldsymbol{w}\|^2_{\partial T,1/2}\right)^{1/2} |||e||| \tag{53}$$

Finally, the following inequality, see Larson and Målqvist [10] for a detailed proof, holds

$$\inf_{\boldsymbol{w}\in[C(\Omega)]^2} \sum_{T\in\mathcal{T}} \|\nabla U - \boldsymbol{w}\|^2_{\partial T,1/2} \leq C\sum_{T\in\mathcal{T}} h_T^{-1}\|[\nabla U]\|^2_{\partial T} \tag{54}$$

and thus we finally obtain the estimate

$$III \leq C\left(\sum_{T\in\mathcal{T}} h_T^{-1}\|[\nabla U]\|^2_{\partial T}\right)^{1/2} |||e||| \tag{55}$$

Collecting the estimates of terms I–III the theorem follows. □

4 Numerical Examples

4.1 Adaptive Refinement for a Point Load

We consider a plate covering the domain $\Omega = (0,1) \times (0,1)$ and carrying a point load situated at $(0.75, 0.625)$. The plate is simply supported, i.e., $u = 0$ on $\partial\Omega$, and the material data are $E = 1$, $\nu = 0.5$, and the thickness is $t = 0.1$. A Fourier series solution to this problem can be found, e.g., in [11]. For our numerical solution we use a $\mathcal{CP}_2$ approximation.

We show a sequence of refined meshes in Figures 1–2, and the variation of the effectivity index, defined as

$$\text{Eff} := \frac{\sqrt{C \sum_{T \in \mathcal{T}} \eta_T^2}}{|||u - U|||}$$

where we arbitrarily set $C = 10$, is shown in Figure 3. This example serves to show that Eff remains fairly constant during the adaptive process. The refinement levels are the same as those referred to in Figures 1–2.

4.2 Locking for the $\mathcal{CP}_2$ Approximation

As is well known, nodally based piecewise C^1–approximations on general meshes require at least quintic polynomials. In the current framework, this is manifested as a mesh sensitivity of the scheme with respect to the parameter γ_0 for low order k. If γ_0 is chosen too large, locking will occur unless a globally C^1 approximation is contained in the approximation space. We show the difference in sensitivity for a $\mathcal{CP}_2$ approximation on three different types of meshes, and compare with the Morley approximation in Figures 4–6. The domain and material data are as above, we use a uniform load, and show the the midpoint displacement as a function of γ_0, with the exact solution and the Morley solution as a reference. We note that on the criss-cross mesh, the solution is robust with respect to locking (which can be explained by the existence of a C^1 approximation on this type of mesh, see [16]), and less stiff than the Morley element. In case of an unstructured mesh we see a slightly stronger locking tendency, and for the directional mesh it is distinct. We conclude that γ_0 must be chosen judiciously in the case of $\mathcal{CP}_2$ approximations. We also note that the optimal γ_0 depends on the mesh.

References

[1] G. A. Baker. Finite element methods for elliptic equations using nonconforming elements. *Math. Comp.*, 31(137):45–59, 1977.

[2] R. Becker, P. Hansbo, and M. G. Larson. Energy norm a posteriori error estimation for discontinuous Galerkin methods. *Comput. Methods Appl. Mech. Engrg.*, 192(5-6):723–733, 2003.

[3] L. Beirão da Veiga, J. Niiranen, and R. Stenberg. A posteriori error estimates for the Morley plate bending element. *Numer. Math.*, 106(2):165–179, 2007.

[4] S. Brenner, R.L Scott, *The Mathematical Theory of Finite Element Methods*, Springer, New York, 1994.

[5] C. Carstensen, S. Bartels, and S. Jansche. A posteriori error estimates for nonconforming finite element methods. *Numer. Math.*, 92(2):233–256, 2002.

[6] P. G. Ciarlet. *The Finite Element Method for Elliptic Problems.* North-Holland, Amsterdam, 1978.

[7] E. Dari, R. Duran, C. Padra, and V. Vampa. A posteriori error estimators for nonconforming finite element methods. *RAIRO Modél. Math. Anal. Numér.*, 30(4):385–400, 1996.

[8] G. Engel, K. Garikipati, T. J. R. Hughes, M. G. Larson, L. Mazzei, and R. L. Taylor. Continuous/discontinuous finite element approximations of fourth-order elliptic problems in structural and continuum mechanics with applications to thin beams and plates, and strain gradient elasticity. *Comput. Methods Appl. Mech. Engrg.*, 191(34):3669–3750, 2002.

[9] P. Hansbo and M. G. Larson. A discontinuous Galerkin method for the plate equation. *Calcolo*, 39(1):41–59, 2002.

[10] M. G. Larson and A. Målqvist. A posteriori error estimates for mixed finite element approximations of elliptic problems. *Numer. Math.*, 108(3):487–500, 2008.

[11] E. H. Mansfield. *The Bending and Stretching of Plates*, 2:nd ed. Cambridge University Press, Cambridge, 1989.

[12] L. S. D. Morley. The triangular equilibrium element in the solution of plate bending problems. *Aero. Quart.*, 19:149–169, 1968.

[13] V. Thomée. *Galerkin Finite Element Methods for Parabolic Problems.* Springer-Verlag, Berlin, 1997.

[14] T. Warburton and J.S. Hesthaven. On the constants in *hp*–finite element trace inverse inequalities. *Comput. Methods Appl. Mech. Engrg.* 192:2765–2773, 2003.

[15] G. N. Wells and N. T. Dung. A C^0 discontinuous Galerkin formulation for Kirchhoff plates. *Comput. Methods Applied Mech. Engrg.*, 196:3370–3380, 2007.

[16] S. Zhang. A C1-P2 finite element without nodal basis, *ESAIM: Math. Model. Numer. Anal.* (to appear).

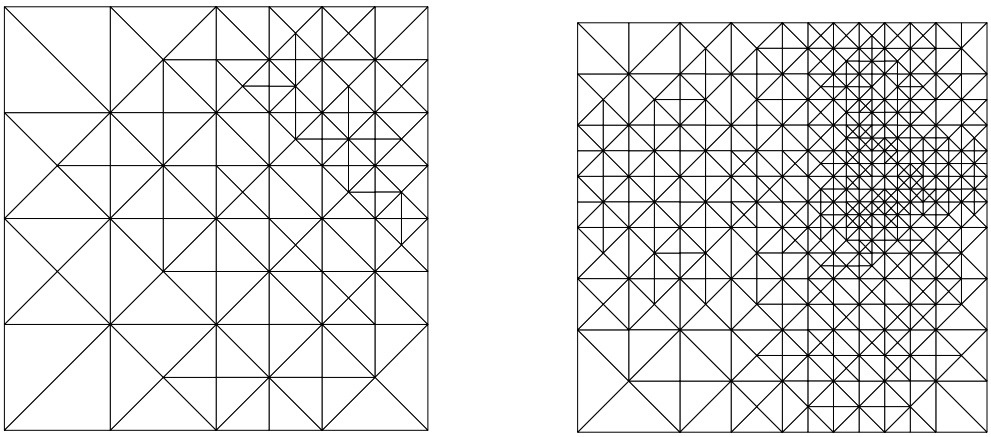

Figure 1: Adapted meshes after 5 and 10 refinement levels

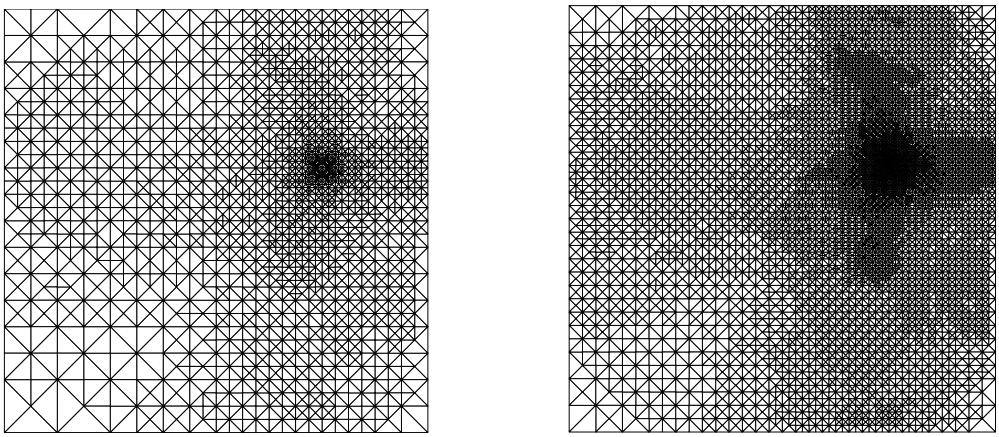

Figure 2: Adapted meshes after 15 and 20 refinement levels

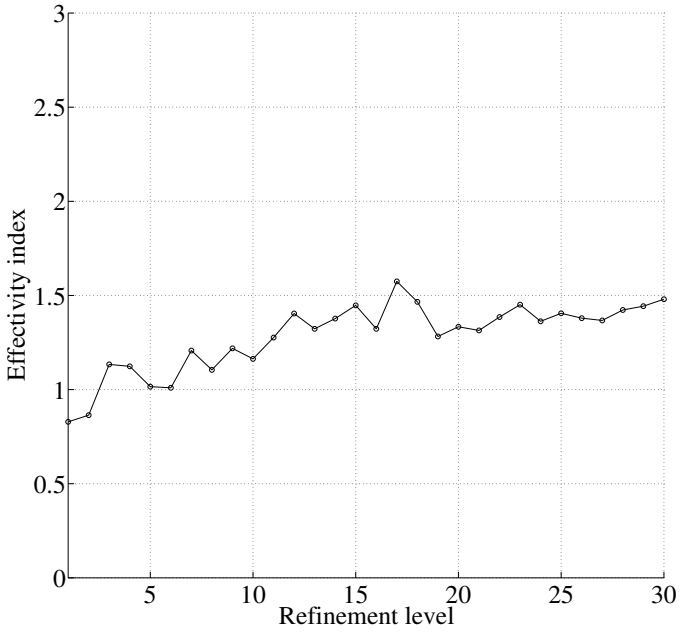

Figure 3: Variation of the effectivity index

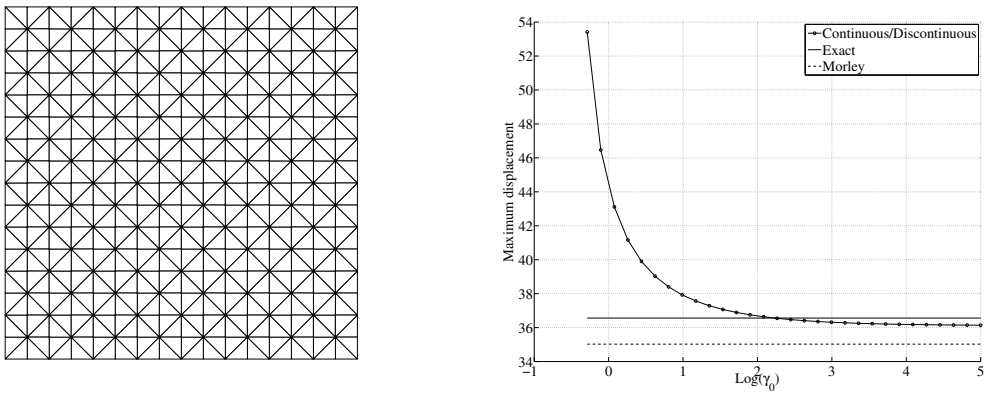

Figure 4: A criss-cross mesh and sensitivity with respect to γ_0

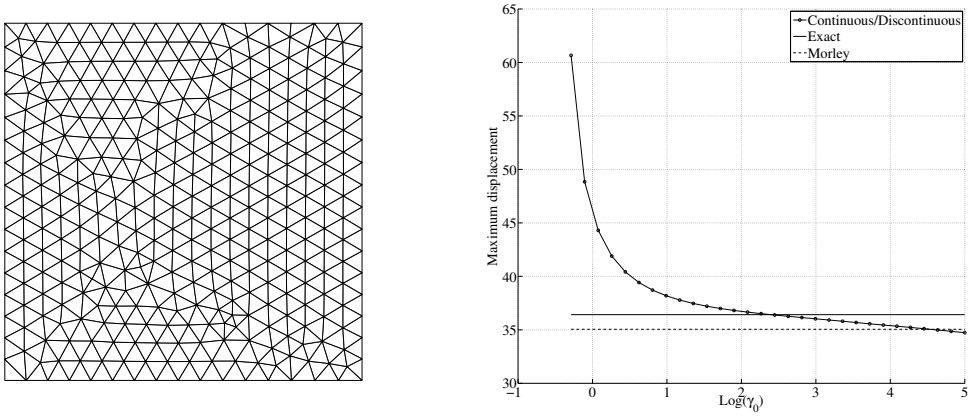

Figure 5: An unstructured mesh and sensitivity with respect to γ_0

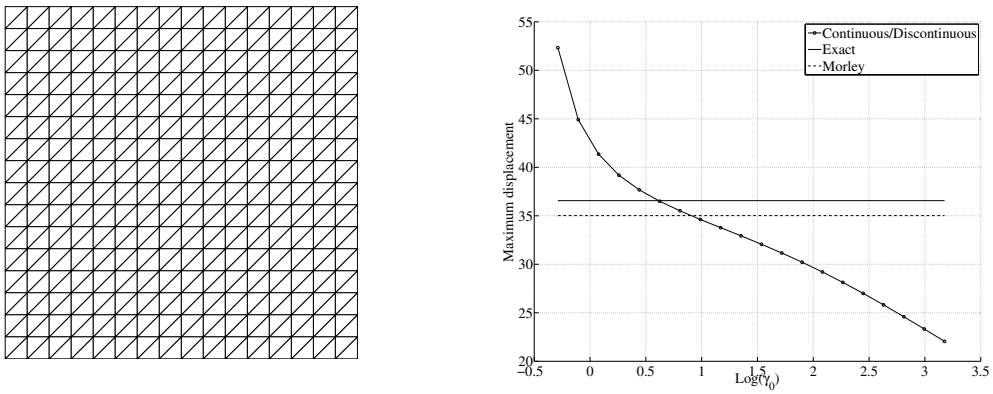

Figure 6: A mesh with directionality and sensitivity with respect to γ_0